Er^{3+} luminescence and cooperative upconversion in $Er_xY_{2-x}SiO_5$ nanocrystal aggregates fabricated using Si nanowires

Kiseok Suh,[1] Jung H. Shin,[1,a)] Seok-Jun Seo,[2] and Byeong-Soo Bae[2]
[1]*Department of Physics, Korea Advanced Institute of Science and Technology (KAIST), 373-1 Guseong-dong, Yuseong-gu, Daejeon, Republic of Korea*
[2]*Department of Materials Science and Engineering, Korea Advanced Institute of Science and Technology (KAIST), 373-1 Guseong-dong, Yuseong-gu, Daejeon, Republic of Korea*

(Received 19 July 2007; accepted 8 February 2008; published online 26 March 2008)

Er^{3+} luminescence and cooperative upconversion in $Er_xY_{2-x}SiO_5$ nanocrystal aggregates fabricated using Si nanowires is investigated. X-ray diffraction and photoluminescence spectroscopy indicate that the composition of the final nanocrystals can be varied continuously from pure Y_2SiO_5 to pure Er_2SiO_5 while keeping the crystal structure the same. Analysis of concentration and pump-power dependence of the Er^{3+} photoluminescence intensity and decay time shows that while cooperative upconversion occurs at high Er concentrations, the cooperative upconversion coefficient is only $(2.2\pm1.1)\times10^{-18}$ cm^3/s at a Er concentration of 1.2×10^{21} cm^{-3}. This is nearly ten times lower at more than ten times higher Er concentration than that reported from Er-doped silica and demonstrates the viability of using such silicates for compact, high-gain Si-based optical material for Si photonics. © *2008 American Institute of Physics*. [DOI: 10.1063/1.2890414]

The ever-increasing level of integration and ever-decreasing device sizes in Si integrated circuits has led to the emergence of "interconnect bottleneck," in which the *RC* delay and heat generation due to the metal interconnects become the limiting factor for the actual performance of Si integrated circuits.[1] One proposed solution to this problem is integration of photonic devices to realize fast, lossless optical inter- and intrachip communications to fundamentally remove problems associated with metal interconnects.[1] By now, intense research effort has led to demonstration of many important components such as >10 Ghz modulators,[2] optical buffers,[3] and compact detectors.[4]

However, one key component whose development has been relatively modest is a Si-based compact optical amplifier that can overcome the inherent limitation of the indirect band gap of Si. Of the many approaches,[5] using Er^{3+} ion as an optical dopant has attracted a special attention because of its ability to provide light at 1.5 μm that is compatible with both silicon-on-insulator based Si microphotonic devices and optical telecommunication.[1]

Unfortunately, the emission cross section and solubility of Er^{3+} in silica are $<10^{-20}$ cm^2 and $\sim10^{20}$ cm^{-3}, respectively, resulting in optical gain of a few dB/cm only. This results in large amplifiers that are difficult to integrate into a compact device. Recently, however, many researchers have shown that by increasing the Er concentration to such a degree that Er silicate phases can form, the concentration of optically active Er can be increased to more than 10^{22} cm^{-3}, enabling, in principle, optical gain in excess of several hundred dB/cm.[6–8] In reality, however, such a high concentration leads to cooperative upconversion (CU) that limits the possible gain.[9] Therefore, characterizing and controlling Er^{3+} luminescence and upconversion in such Er silicates are necessary in order to utilize them for amplifier applications.

In this paper, we report on Er^{3+} luminescence and CU in $Er_xY_{2-x}SiO_5$ nanocrystal aggregates. Y_2SiO_5 has lattice constants that are nearly identical to that of Er_2SiO_5,[10] which should allow uniform dilution of Er by Y. Analysis shows that while CU occurs at high Er concentrations, the CU coefficient (CUC) is only $(2.2\pm1.1)\times10^{-18}$ cm^3/s at a Er concentration of 1.2×10^{21} cm^{-3}. This is nearly ten times lower at more than ten times higher Er concentration than that reported from Er-doped silica and demonstrates the viability of using such silicates for compact, high-gain Si-based optical material for Si-photonics.

$Er_xY_{2-x}SiO_5$ nanocrystals were fabricated by spin coating $YCl_3\cdot6H_2O$ and $ErCl_3\cdot6H_2O$ dissolved ethanol solution on a dense array of Si nanowires and subsequently rapid thermal annealing them at 900 °C for 4 min in a flowing N_2/O_2 environment and then at 1200 °C for 5 min in a flowing Ar environment. Detailed description of the fabrication process can be found in Ref. 7. The nominal Er concentrations, as intended by the reactant ratio, were 0 (i.e., pure Y_2SiO_5), 0.26, 1, 5, 10, 18, and 25 at. % (i.e., pure Er_2SiO_5) Er. These values, except for 0.26 at. % due to the detection limit, were confirmed by energy-dispersive x-ray spectroscopy to be 1.5, 5, 8.8, 17, and 25 at. %. Photoluminescence (PL) spectra were obtained using the 488 nm line of an Ar laser, a grating monochromator, and employing the standard lock-in technique. The pump beam size, as determined using a complementary metal-oxide semiconductor image sensor, was 0.15 mm^2. The PL decay traces were collected to digitized oscilloscope.

Figure 1 shows the x-ray diffraction (XRD) spectra from fabricated nanocrystals. The reported peak positions of Er_2SiO_5 and Y_2SiO_5 are also indicated.[10] We observe identical spectra from all samples ranging from pure Y_2SiO_5 to pure Er_2SiO_5, with peaks that agree well with the reported peak positions. The inset shows typical transmission-electron micrsocopy (TEM) and high-resolution TEM images of the fabricated nanocrystals, showing hundred-nanometer sized, single-crystalline grains.

Figure 2 shows the near-infrared PL spectra from the fabricated nanocrystals, normalized to the intensity at 1.53 μm. The shape of the PL peak near 1.53 μm due to $^4I_{13/2}\rightarrow{}^4I_{15/2}$ transition is the same for all Er concentrations

a)Electronic mail: jhs@kaist.ac.kr.

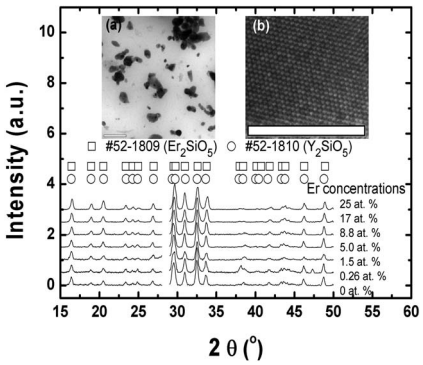

FIG. 1. X-ray diffraction spectra of fabricated nanocrystal aggregates. The peak positions from JCPDS powder diffraction are indicated by open square (Er_2SiO_5) [Ref. 10(a)] and open circle (Y_2SiO_5) [Ref. 10(b)] for comparison. The inset shows the typical TEM and high-resolution TEM images of fabricated nanocrystal aggregates, also shown at the size and single-crystalline quality of individual grains. The scale bar for TEM image represents 500 nm, while the scale bar for the high-resolution TEM represents 10 nm.

and is very similar to previously reported PL spectra from similar, Er silicate thin films.[11] The intra-4*f* transitions of Er^{3+} are parity forbidden but become allowed by the crystal field and, therefore, reflect the local atomic structure of Er^{3+}. Thus, the fact that we observe the same sharp PL spectra for all Er concentrations, together with the XRD spectra shown in Fig. 1, clearly demonstrates that the crystal structure of the fabricated $Er_xY_{2-x}SiO_5$ nanocrystals is the same for all Er concentrations, right down to the atomic level. On the other hand, the PL peak near 0.98 μm due to $^4I_{11/2} \rightarrow {}^4I_{15/2}$ transition is observable only for Er concentration of 5.0 at. % or higher, even though the pump power was the same for all samples.

Similar concentration dependence is shown in Fig. 3(a), which shows the decay traces of 1.53 μm Er^{3+} PL intensity for different Er^{3+} concentrations. At Er^{3+} concentration of 0.26 at. %, we observe a single-exponential decay with a luminescent lifetime of 7.4 ms. As the Er concentration is increased further, the decay traces become nonexponential characterized by a fast initial decay. Figure 3(b) shows the decay traces of 1.53 μm Er^{3+} PL intensity from the sample with 1.5 at. % Er at different pump powers. At 2 mW, the decay trace is single-exponential, with a luminescent lifetime of 8 ± 0.5 msec. As the pump power is increased, the decay

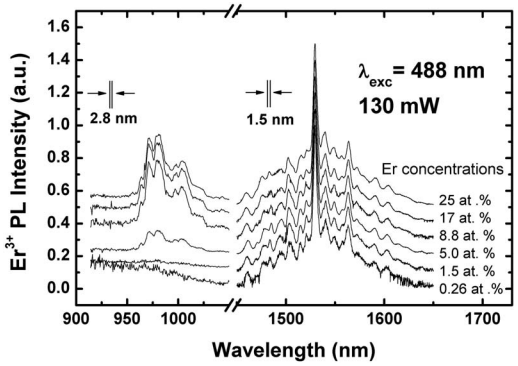

FIG. 2. High-resolution PL spectra of fabricated nanocrystal aggregates using 488 nm line of an Ar laser at room temperature, normalized to the intensity at 1.53 μm. Curves are offset for clarity. Note that 0.98 μm luminescence is observable only for Er concentration of 5.0 at. % or higher, even though the pump power was the same for all samples. The spectral resolutions at around 0.98 and 1.5 μm are 2.8 and 1.5 nm, respectively.

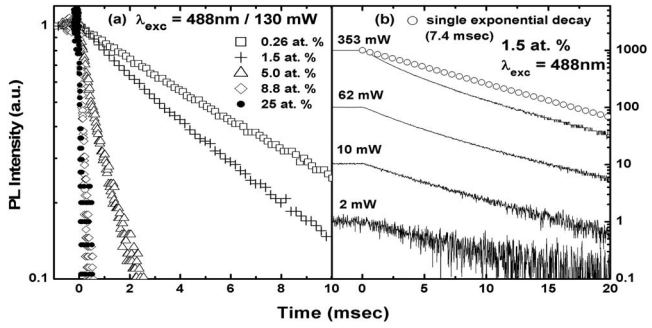

FIG. 3. (a) The decay traces of 1.53 μm Er^{3+} PL intensity for different Er concentrations. As the Er concentration is increased, the decay traces become nonexponential characterized by a fast initial decay. (b) The decay traces of 1.53 μm Er^{3+} PL intensity from the sample with 1.5 at. % Er for different pump powers. As the pump power is increased, the fast initial decay appears.

traces become nonexponential with shorter lifetimes. We note, however, that all decay traces, after the fast, initial decay, approach a single-exponential decay with a luminescent lifetime of 7.4 ms.

Such concentration-dependent 0.98 μm Er^{3+} PL intensity, together with the concentration- and pump-power dependent 1.53 μm Er^{3+} PL decay traces, bears the hallmark of CU, in which a Er^{3+} ion in the first excited state ($^4I_{13/2}$) decays nonradiatively to the ground state ($^4I_{15/2}$) by exciting another Er^{3+} ion in the first excited state to the third excited state ($^4I_{9/2}$), which then thermalizes rapidly to lower-lying states. This is an important loss mechanism that limits optical gain in Er^{3+} based 1.53 μm amplifiers and lasers and must be investigated if $Er_xY_{2-x}SiO_5$ is to be used for optical amplifiers.

First, note that we do not observe 0.98 μm PL peak at low Er concentrations even though we are exciting the 4*f* electrons to the higher-lying $^4F_{7/2}$ level by the 488 nm pump beam. This indicates that the thermalization of the 4*f* electrons down to the $^4I_{13/2}$ level is very rapid, consistent with the high phonon energies reported for rare-earth oxyorthosilicates.[12] Thus, we approximate the 4*f* electron distribution in low Er^{3+} concentration nanocrystals by a two-level model in which we consider the ground and first excited states of Er^{3+} only.[9] In such a case, we can write

$$dn(t)/dt = \sigma\phi(1-n) - n/\tau - CNn^2, \tag{1}$$

where n, σ, ϕ, τ, C, and N are fraction of Er^{3+} in first excited state, the excitation cross section (ECS), pump photon flux, decay lifetime, CUC, and concentration of Er, respectively. The analytic solution of Eq. (1) is[9]

$$n(t) = (1/\tau)\{[1/\tau n(0) + CN]\exp(t/\tau) - CN\}^{-1}, \tag{2}$$

$$n(0) = [(\sigma\phi + 1/\tau)/2CN]\{[1 + 4CN\sigma\phi/(\sigma\phi + 1/\tau)^2]^{1/2} - 1\}. \tag{3}$$

In Eqs. (2) and (3), $n(0)$ represents the steady-state value of n, and $n(t)$ represents the time evolution n at time t after the pump beam has been turned off at $t=0$. As $n(0)$ is proportional to the 1.53 μm Er^{3+} PL intensity, C can be found by fitting Eqs. (2) and (3) to the luminescence decay curve and the pump-power dependence of 1.53 μm Er^{3+} luminescence intensity, provided that σ and τ are known. For τ, we use 7.4 ms, which is the lifetime observed under conditions where CU is negligible. To obtain σ, we have measured the

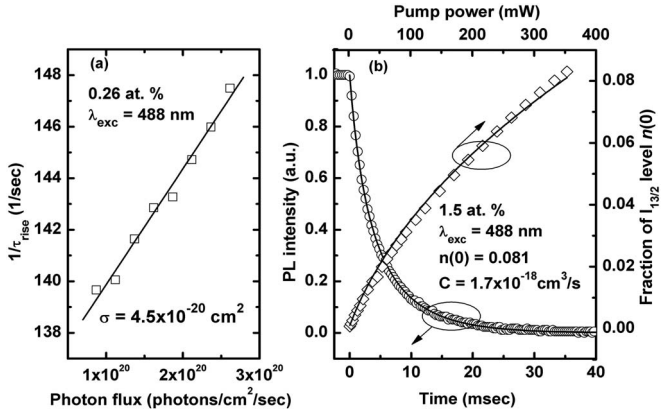

FIG. 4. (a) The risetime of 1.53 μm Er^{3+} PL from the sample with 0.26 at. % Er as a function of photon flux. The solid line is a result of linear fitting to the data. The slope of the line gives the excitation cross section which is 4.5×10^{-20} cm^2. (b) The 1.53 μm Er^{3+} PL intensity as a function of pump power and the decay traces at the pump power of 353 mW from the sample with 1.5 at. % Er. By using a single set of parameters to fit both curves with Eqs. (2) and (3) when $\sigma=4.5\times10^{-20}$ cm^2 is used, we obtain values $C=1.7\times10^{-18}$ cm^3/s and $n(0)=0.081$. The fitting results are shown as the solid curves.

rise time of 1.53 μm Er^{3+} PL from the sample with 0.26 at. % Er at different pump powers, under the condition that no CU effects appear. The results are shown in Fig. 4(a). The slope of the curve then gives σ, which was found to be $(4.5\pm0.2)\times10^{-20}$ cm^2. This value is much higher than the value of $\sim(2-3)\times10^{-21}$ cm^2 typically reported[13] for $^4F_{7/2}$ level of Er^{3+}, which we attribute to the multiple scattering of pump beam by nanocrystal aggregates. We note that the intrinsic value of atomic σ should be the same for all Er concentrations, since the absorption and emission processes of Er^{3+} ions are atomic in nature. A possible source of error, however, is the variation in the detailed structure of the nanocrystal aggregates which can affect the multiple scattering, leading to sample-to-sample variation of the effective ECS used in calculations. To investigate the variation, we measured the Er^{3+} PL properties from more than 30 samples with 2.5 at. % Er and found the variation in the PL intensity to be about $\pm50\%$ and the variation of the Er^{3+} luminescence decay time to be $\pm10\%$ (data not shown). Based on these data, we calculate the ECS of the sample with 1.5 at. % Er to be $(4.5\pm2.3)\times10^{-20}$ cm^2.

Figure 4(b) shows the PL decay curve at the pump power of 353 mW and the pump power dependence of 1.53 μm Er^{3+} PL intensity. By using a single set of parameters to fit both curves to Eqs. (2) and (3) with σ value in the range of $(4.5\pm2.3)\times10^{-20}$ cm^2, we obtain values $C=(2.2\pm1.1)\times10^{-18}$ cm^3/s with $n(0)=0.081\pm0.039$. The fitting result of $C=1.7\times10^{-18}$ cm^3/s with $n(0)=0.081$ (when $\sigma=4.5\times10^{-20}$ cm^2 is used) is shown by solid curves in Fig. 4(b).

This simultaneous achievement of high Er concentration and low value of C is very unusual compared to values reported for other materials. In the case of Er-doped silica, C was reported to be as high as 1.7×10^{-17} cm^3/s at a Er concentration of 1×10^{20} cm^{-3}.[14] A lower value of 3×10^{-18} cm^{-3}/s had been reported for Ge/Al doped fused silica optical fibers[15] but only at a low Er concentration of $\sim2\times10^{19}$ cm^{-3}. A comparable value of 1.2×10^{-18} cm^3/s at a Er concentration of 6×10^{20} cm^{-3} has been reported but in the case of bulk soda-lime silicate glasses prepared from batches melted at 1400 °C for as long as 50 h.[16]

The exact reason for such a low value of C is not yet clear. We postulate, however, that the high crystalline quality of the fabricated $Er_xY_{2-x}SiO_5$ nanocrystals[7] is at least partially responsible, as the crystal structure of oxyorthosilicates has only two sites for rare-earth ions that are separated by either a bridging oxygen or a SiO_4 tetrahedra,[17] and thereby precludes the possibility for formation of Er clusters that are known to lead to high values of C.[18] In addition, the near-perfect lattice matching between Er_2SiO_5 and Y_2SiO_5 allows dilution of Er within the matrix without formation of Er_2SiO_5 domains.

For amplifier applications, it is more likely that 0.98 or 1.48 μm pump beam will be used. However, the exact values of absorption/emission cross section for Er^{3+} in Y_2SiO_5 are not well-known. Taking the reported values of 1.48 μm absorption cross section ($\sim3\times10^{-21}$ cm^2) and 1.53 μm emission cross section of Er^{3+} in silica ($\sim1\times10^{-20}$ cm^2), we can use Fig. 4(b) to estimate that population inversion can be achieved at a pump power of 52 kW/cm^2 and 42 dB/cm gain, corresponding to 90% inversion, can be achieved at a pump power of 800 kW/cm^2.

In conclusion, we have investigated Er^{3+} luminescence and cooperative upconversion in $Er_xY_{2-x}SiO_5$ nanocrystal aggregates fabricated using Si nanowires. Analysis shows that the cooperative upconversion coefficient is only $(2.2\pm1.1)\times10^{-18}$ cm^3/s at a Er concentration of 1.2×10^{21} cm^{-3}. This is nearly ten times lower at ten times higher Er concentration than that reported from Er-doped silica, and demonstrates the viability of using such silicates for compact, high-gain Si-based optical material for Si-photonics.

This work was supported in part by NRL and by Grant No. (R11-2003-022) from OPERA of the Korea Science and Engineering Foundation.

[1]See, for example, *Silicon Photonics*, Topics in Applied Physics Vol. 94 (Springer, Berlin, 2004).
[2]Q. Xu, S. Manipatruni, B. Schmidt, J. Shakya, and M. Lipson, Opt. Express **15**, 430 (2007).
[3]F. Xia, L. Sekaric, and Y. Vlasov, Nat. Photonics **1**, 65 (2007).
[4]D. Ahn, C.-Y. H. J. Liu, W. Giziewicz, M. Beals, L. C. Kimerling, J. Michel, J. Chen, and F. X. Kärtner, Opt. Express **15**, 3916 (2007).
[5]H. S. Rong, R. Jones, A. S. Liu, O. Cohen, D. Hak, A. Fang, and M. Paniccia, Nature (London) **433**, 725 (2005).
[6]M. Miritello, R. L. Savio, F. Iacona, G. Franzó, A. Irrera, A. M. Piro, C. Bongiorno, and F. Priolo, Adv. Mater. (Weinheim, Ger.) **19**, 1582 (2007).
[7]K. Suh, J. H. Shin, S.-J. Seo, and B.-S. Bae, Appl. Phys. Lett. **89**, 223102 (2006).
[8]H.-J. Choi, J. H. Shin, K. Suh, H.-K. Seong, H.-C. Han, and J.-C. Lee, Nano Lett. **5**, 2432 (2005).
[9]E. Snoeks, G. N. van den Hoven, A. Polman, B. Hendriksen, M. B. J. Diemeer, and F. Priolo, J. Opt. Soc. Am. B **12**, 1468 (1995).
[10](a) JCPDS Card No. 52-1809 (unpublished); (b) JCPDS Card No. 52-1810 (unpublished).
[11]H. Isshiki, A. Polman, and T. Kimura, J. Lumin. **102-103**, 819 (2006).
[12]L. Fornasiero, K. Petermann, E. Heumann, and G. Huber, Opt. Mater. (Amsterdam, Neth.) **10**, 9 (1998).
[13]W. J. Miniscalco, J. Lightwave Technol. **9**, 234 (1991).
[14]M. Federighi and F. Di Pasquale, IEEE Photonics Technol. Lett. **7**, 303 (1995).
[15]J. Nilsson, P. Blixt, B. Jaskorzynska, and J. Babonas, J. Lightwave Technol. **13**, 341 (1995).
[16]M. P. Hehlen, N. J. Cockroft, T. R. Gosnell, A. J. Bruce, G. Nykolak, and J. Shmulovich, Opt. Lett. **22**, 772 (1997).
[17]J. Felsche, Struct. Bonding (Berlin) **13**, 99 (1973).
[18]P. G. Kik and A. Polman, J. Appl. Phys. **93**, 5008 (2003).